

## Controlled Dephasing of an Electron Interferometer with a Path Detector at Equilibrium

E. Weisz, H. K. Choi, M. Heiblum,\* Yuval Gefen, V. Umansky, and D. Mahalu

*Braun Center for Submicron Research, Department of Condensed Matter Physics,  
Weizmann Institute of Science, Rehovot 76100, Israel*

(Received 5 June 2012; published 18 December 2012)

Controlled dephasing of electrons, via “which path” detection, involves, in general, coupling a coherent system to a current driven noise source. However, here we present a case in which a nearly isolated electron puddle within a quantum dot, at thermal equilibrium and in millikelvin range temperature, fully dephases the interference in a nearby electronic interferometer. Moreover, the complete dephasing is accompanied by an abrupt  $\pi$  phase slip, which is robust and nearly independent of system parameters. Attributing the robustness of the phenomenon to the Friedel sum rule—which relates a system’s occupation to its scattering phases—proves the universality of this powerful rule. The experiment allows us to peek into a nearly isolated quantum dot, which cannot be accessed via conductance measurements.

DOI: [10.1103/PhysRevLett.109.250401](https://doi.org/10.1103/PhysRevLett.109.250401)

PACS numbers: 03.65.Yz, 03.65.Ud, 07.60.Ly

Coherence and dephasing of quantum systems is of great interest for both practical and theoretical reasons. Controlled dephasing has been studied in different mesoscopic systems in order to understand the important parameters that govern coherence. Most of the works concentrated on coupling a coherent system to a noisy, current driven, source (serving as “path detector”), which led to partial or full dephasing of the system [1–5]. Here, we present a setup in which a coherent Fabry-Perot interferometer, in form of an unbiased, nearly pinched, quantum dot (QD), bathed in 45 mK temperature, induces full dephasing in a nearby two-path electronic Mach Zehnder interferometer (MZI) [6]. Aside from the remarkable, and unexpected, dephasing of the MZI by the stagnant QD, observing the visibility and phase of the MZI teaches us on the inwards of a pinched QD.

Our setup consisted of an electronic MZI strongly coupled to a QD. This complex was realized using the chiral edge channels formed in a two-dimensional electron gas (2DEG) (electron density  $n = 2.7 \times 10^{11} \text{ cm}^{-2}$ , mobility  $\mu = 2.5 \times 10^6 \text{ cm}^2/\text{V s}$ ) in the integer quantum Hall regime (Fig. 1). Operating in filling factor  $\nu = 2$ , the MZI (active area  $A = 6 \times 6 \mu\text{m}^2$ ) was formed using the outer channel (red), while the QD (lithographic area  $A = 0.4 \times 0.4 \mu\text{m}^2$ , with charging energy  $E_C \approx 100 \mu\text{eV}$  and level spacing  $\Delta E \approx 20 \mu\text{eV}$ ) was formed with the inner edge channel (black). The proximity of the two edge channels ensured strong electrostatic coupling between the MZI and the QD. Differential conductance measurements at  $D1$  were performed in a dilution refrigerator ( $T = 45 \text{ mK}$ ), using an excitation signal of  $3 \mu\text{V}$  rms at 865 kHz, amplified *in situ* by a homemade preamplifier (voltage gain 5) and a room temperature amplifier (gain 200), to be finally monitored by a spectrum analyzer.

The beam splitters in the optical MZI were replaced in our electronic MZI by quantum point contacts QPC1 and QPC2 (Fig. 1), which partitioned the outer edge channel while fully reflecting the inner channel. The phase dependent transmission of the MZI to  $D1$  can be expressed as

$$\begin{aligned} T_{\text{MZI}} &= |t_1 t_2 + e^{i\phi_{\text{AB}}} r_1 r|^2 \\ &= |t_1 t_2|^2 + |r_1 r|^2 + 2t_1 t_2 r_1 r \cos\phi_{\text{AB}} \\ &= T_0 + T_\phi \cos\phi_{\text{AB}}, \end{aligned}$$

with  $\nu = T_\phi/T_0$  the visibility,  $r$  and  $t$  are the reflection and transmission amplitudes of the QPCs, and  $\phi_{\text{AB}} = 2\pi\Delta\Phi/\Phi_0$  is the Aharonov-Bohm (AB) phase, where  $\Phi_0 = h/e$  is the flux quantum; the transmission to  $D2$  is  $1 - T_{\text{MZI}}$ . The AB phase is controlled by altering the magnetic flux enclosed by the two paths of the MZI using the “modulation gate” (MG). An additional QPC0, located upstream of the system, allowed separate sourcing of the outer and inner channels from distant Ohmic contacts  $S1$  and  $S2$ , respectively.

The electrostatic gates forming the QPCs of the QD (QDF, QDL, QDR), were charged so to *fully pass* the outer channel while forming a confined puddle of the inner edge channel within the QD, being Coulomb blocked due to its small capacitance. The potential of the puddle, and hence its occupation, was controlled by charging QDP, known as the “plunger gate.” The confined electron puddle is quantized with levels separation  $\Delta E \approx 20 \mu\text{eV}$  and charging energy is  $E_C \approx 100 \mu\text{eV}$ .

Optimal conditions were obtained via charging appropriately the defining gates. The MZI transmission experienced AB oscillations when modulated by  $V_{\text{MG}}$ . Repeating this measurement over a range of puddle occupations, controlled by  $V_{\text{QDP}}$ , the data were analyzed by means of

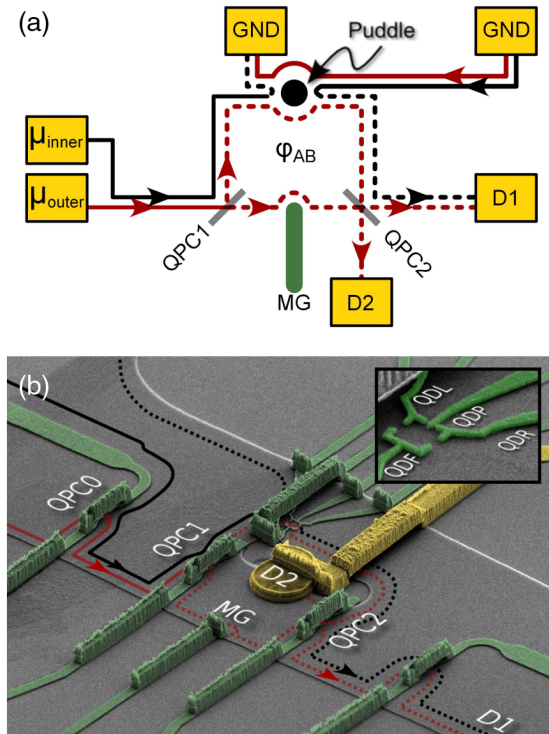


FIG. 1 (color online). Schematics and SEM picture of the studied system. (a) The system comprises an electronic MZI of the chiral outer edge mode in the integer quantum Hall effect in filling factor 2 (red) and a quantum dot interferometer, in the Coulomb blockade regime, of the chiral inner edge mode (black). Full lines represent full beams; dashed lines represent partitioned beams. The electron puddle lies between the two outer edge modes, one is serving as the upper arm of the MZI and the other returning from the grounded contact. The puddle is coupled capacitively and quantum mechanically to all four edge modes. When tunneling is effective, it is only via the inner edge mode. (b) A scanning electron microscope micrograph of the fabricated structure, which was realized in a GaAs/AlGaAs heterostructure embedding a two dimensional electron gas by employing photolithography and electron beam lithography techniques. The trajectories of the outer (red) and inner (black) edge modes were defined by etching and biasing surface gates (green). Ohmic contacts serve as drain  $D1$  (not seen) and  $D2$  (yellow). Measurements were conducted at an electron temperature of  $\sim 45$  mK and at a magnetic field of 5.6 T.

a fast Fourier transform, yielding the transmission, the visibility and the phase of the MZI.

We first discuss the results for a QD relatively well coupled to the leads, namely the inner edge channels impinging from left and right. The conductance of the QD,  $G_{\text{QD}}(\text{QDP})$ , peaks periodically, with peaks separated by regions of negligible conductance; This is the well-known Coulomb blocked regime. Figure 2(a) shows the conductance of the MZI-QD complex as measured at  $D1$ , comprised of the QD's Coulomb peaks on top of the MZI's average conductance of  $0.5e^2/h$ . In the MZI, every conductance peak is accompanied by a visibility dip

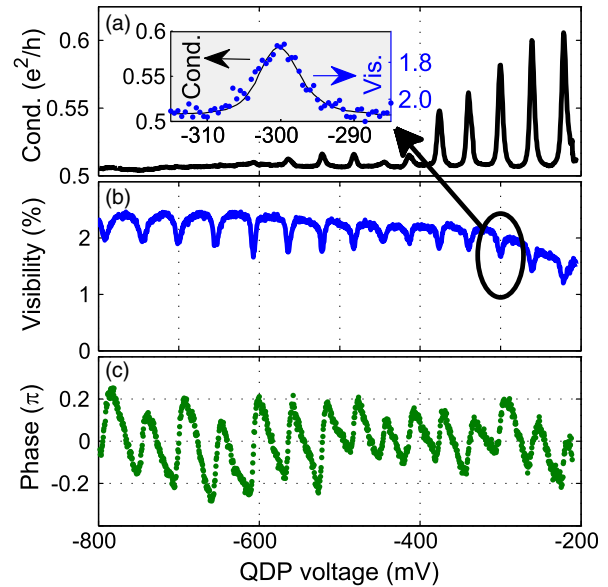


FIG. 2 (color online). Conductance peaks of the QD, visibility, and phase of the MZI ( $B = 5.6$  T). (a) Coulomb blockade peaks of the QD (each peak maximum is at the degeneracy point of  $N$  and  $N + 1$  electrons in the QD). (b),(c) The visibility of the interference oscillations quenches and the oscillation phase undergoes a lapse at the degeneracy points. As the coupling of the QD to the leads is increased (affected inadvertently by the plunger gate voltage), the phase lapses widen and diminish while the visibility dips become shallower. Identical results were observed when the QD was at thermal equilibrium. The inset in (a) compares the line shape of a visibility dip with that of the corresponding Coulomb blockade peak (both Lorentzian).

[Fig. 2(b)] and a sharp slip in the AB phase [Fig. 2(c)]. Note that the visibility follows qualitatively accurately the conductance [inset, Fig. 2(a)]—being thus a measure of the puddle's occupation. Emptying the dot further (via  $V_{\text{QDP}}$ ), inadvertently pinches QPC1 and QPC2, and thus, quenches the conductance peaks. Yet, the visibility dips in the MZI persist.

Pinching the two QPCs further, thus decoupling the QD from its leads, resulted in deeper visibility dips (i.e., stronger dephasing) and larger, and more abrupt, phase slips. For a nearly isolated QD (namely, without measurable current), the visibility dips drop to zero and the phase slips reach a full  $\pi$  (Fig. 3, Supp. Fig. 1 in [7]). This response of the MZI to a pinched QD, proved to be extremely robust, namely, it persisted at different QD's setups, different magnetic fields, and even in different devices (initial visibility, however, depends on the magnetic field and the setup; see Supp. Fig. 2 [7]). It is important to note that these results were observed when the QD was unbiased, *at an equilibrium*  $T \sim 45$  mK.

Since the line shape of the visibility dips was found to be identical to that of the corresponding QD conductance peaks, level broadening  $\Gamma$  was also reflected in the visibility dips; moreover, this holds also for the corresponding

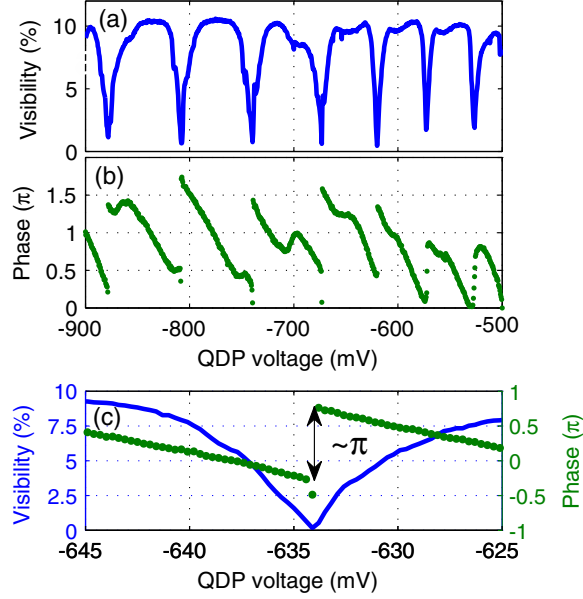


FIG. 3 (color online). The visibility (a) and the oscillations phase (b) for a nearly isolated QD ( $B = 6.3$  T). Visibility is almost completely lost while the phase goes through an abrupt  $\pi$  lapse at the degeneracy points. This is a direct consequence of the Friedel sum rule [9], which ties the scattering phase of a system to its occupation. (c) A detailed view of the vicinity of a single degeneracy point measured at high sensitivity, exhibiting a complete visibility quench and an abrupt  $\pi$  phase lapse.

pinched QD. Plotting the full width at half minimum (FWHM) of the *visibility dips* as a function of the puddle’s coupling to the leads, yielded a surprising result (Fig. 4). While in the coupled regime *the FWHM* decreases and saturates at  $\Gamma < k_B T$  at  $\sim 3.5k_B T$  as the dot was pinched [8], thereafter, surprisingly, it increased linearly with the dwell time, reaching some  $80 \mu\text{eV}$  for dwell times on order of  $1 \mu\text{s}$ .

A model based on Coulomb interactions can account for the observed results. The QDP voltage and the occupation of the QD determine the puddle’s potential, thus “gating” the outer edge channel flowing nearby—distorting its

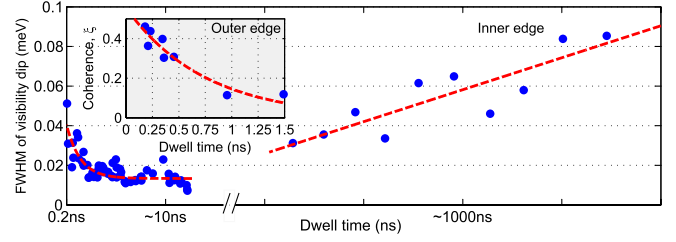


FIG. 4 (color online). Exploring the level width of the QD in the pinched off regime. For a QD coupled to the leads the width of the visibility dips follows the conductance peaks [inset, Fig. 2(a)]. The deduced typical dwell time is  $\tau_{\text{dwell}} = 100$  ps. As the coupling weakened, with  $\tau_{\text{dwell}} \sim 10$  ns, the conductance peaks and visibility dips widths became limited by the electron temperature of  $\sim 45$  mK. Strongly pinching off the QD, transport through the puddle in the QD diminished, leading to a long dwell time—roughly estimated  $\tau_{\text{dwell}} \sim 1 \mu\text{s}$ . The visibility dips widened at this regime, suggesting that inelastic processes come into play increasing the inelastic width, with decoherence time  $\tau_{\text{decoh}} \sim 50$  ps; alternatively, spin-flip processes may allow tunneling to the leads through the outer edge, reducing  $\tau_{\text{dwell}}$ . The inset shows the dependence of the degree of coherence of the QD on the dwell time (measured with the outer edge mode)—with the QD essentially incoherent for  $\tau_{\text{dwell}} > 1$  ns. The red dashed lines serve as guides to the eye.

trajectory and thus shifting the AB phase in the MZI. Alternatively, the dot’s potential has a saw tooth like dependence on the plunger gate voltage [8]: with initial increasing of  $V_{\text{QDP}}$ , Coulomb blockade prevents the entrance of a new electron into the dot, allowing thus an increase of dot’s potential. When the dot’s potential reaches  $e/C$ , with  $C$  the dot’s capacitance, an electron may enter the dot and screen the plunger gate’s charge, thus lower the dot’s potential (on the scale of  $\Gamma$ ). In the time domain, the degeneracy between  $N$  and  $N + 1$  electrons in the dot leads to fluctuations of the electron-number and thus also in the potential of the puddle. Consequently, the AB phase of the MZI will fluctuate between  $\varphi_N$  and  $\varphi_{N+1}$ . A simple model of phasor addition yields the observed visibility and phase of the MZI:

$$v(P_N, P_{N+1}, \Delta\phi) = \left| \sum_{k=N, N+1} P_k e^{i\phi_k} \right| = \sqrt{P_N^2 + P_{N+1}^2 + 2P_N P_{N+1} \cos\Delta\phi}$$

$$\Delta\phi_{\text{MZI}}(P_N, P_{N+1}, \Delta\phi) = \arg\left( \sum_{k=N, N+1} P_k e^{i\phi_k} \right) = \tan^{-1}\left( \frac{P_{N+1} \sin\Delta\phi}{P_N + P_{N+1} \cos\Delta\phi} \right),$$

with  $P_N$  the probability of occupancy  $N$ ,  $\Delta\phi = \varphi_{N+1} - \varphi_N$  and  $\Delta\phi_{\text{MZI}}$  is the observed (average) phase difference. As the charge on the QDP varies smoothly, so does the dot’s potential, consequently affecting the AB phase (Fig. 2). Since we observe a robust phase slip  $\Delta\phi_{\text{MZI}} = \pi$  at the exact resonance, it is obvious why the visibility drops

to zero (i.e.,  $P_N = P_{N+1} = 0.5$ ). This model is further supported by results obtained in the nonlinear regime of the QD, as seen in the Supplemental Material [7].

We attribute the robustness of  $\Delta\phi = \pi$ , which was observed under various conditions in different samples, to the Friedel sum rule [9]. In the context of a two

dimensional electron system, the Friedel rule connects the scattering matrix of an impurity  $S$  to the occupancy of its  $n$  states:  $2\pi i n = \text{Tr}(\ln S)$ . In our system, this rule suggests that adding an electron to the enclosed puddle would be screened by an electron in the two outer edge channels that freely pass the QD (assuming they are the closest “conductors” to the puddle). The total scattering phase would gain  $\Delta\varphi_{\text{top edge}} + \Delta\varphi_{\text{bottom edge}} = 2\pi$  for an added electron. Since the QD is rather symmetric (top-bottom) it is reasonable to assume that the two outer edge channels equally share this phase, namely,  $\Delta\varphi_{\text{top}} = \Delta\varphi_{\text{bottom}} = \pi$ .

The Friedel sum rule can also account, qualitatively, for the reduction in the phase slips and the weaker visibility dips when the QD is strongly coupled to the leads (Fig. 2). The inner edge channels, in this case, approach the confined puddle, thus sharing the screening of an added electron, as well as hosting a fraction of the electron wave function which tunnels out of the dot. The  $2\pi$  phase slip for an added electron is now shared among the outer and inner edge channels, leaving for the lower outer edge channel (upper path of the interferometer) a smaller phase slip, namely,  $\Delta\varphi_{\text{bottom}} < \pi$ .

Monitoring  $\Gamma$ , via the visibility dips, provides unique information of the actual dwell time of electrons in the isolated puddle of electrons. The level width,  $\Gamma = \Gamma_{\text{elas}} + i\Gamma_{\text{inelas}}$ , depends on the dwell time of electrons in the dot (via  $\Gamma_{\text{elas}}$ ), as well as their coherence life time (via  $\Gamma_{\text{inelas}}$ ) [10]. In order to express the FWHM of the visibility dips in terms of energy, the leveraging factor,  $\alpha = \Delta u/e\Delta V_{\text{QDP}} = C_{\text{QDP}}/C_{\text{tot}}$  where  $\Delta u$  is the change in QD potential induced by a change  $\Delta V_{\text{QDP}}$  in plunger gate potential, has to be determined. As the QD pinches, its capacitance to the environment,  $C_{\text{tot}}$ , decreases while the capacitance to the plunger gate,  $C_{\text{QDP}}$ , remains nearly the same resulting in an increase of the leveraging factor. While in the strongly coupled regime  $\alpha = 0.0025$  (determined from the nonequilibrium differential conductance of the QD—the “Diamond Structure” [8]), in the pinched regime we found  $\alpha = 0.015$ , with the bias applied between the lower and upper outer edges (serving as “source” and “drain”; see Supplemental Material).

For a strongly coupled QD, levels are broad, with  $\Gamma_{\text{elas}} \approx 40 \mu\text{eV} \gg k_B T$ , suggesting a dwell time of  $\tau \approx 100$  ps. As the QD is being pinched, the energy levels narrow, and for  $\Gamma_{\text{elas}} \ll k_B T$  the apparent levels’ width is limited by temperature to  $3.5k_B T$ . At this range, the dwell time can be estimated from the height of the conductance peaks, being proportional to  $\Gamma_{\text{elas}}/T$ , with dwell time approaching  $\tau \approx 10$  ns. However, unexpectedly, pinching the QD even further, beyond a dwell time of  $1 \mu\text{s}$ , the apparent FWHM increases monotonically with pinching the QD up to  $80 \mu\text{eV}$ , showing no signs of saturation. This result suggests that at that regime either dwell time is getting shorter or decoherence takes place, effectively

increasing  $\Gamma$ . Being inelastic implies a decoherence time as low as  $\tau_{\text{decoh}} = 50$  ps, with a steady *increase* of the rate with pinching the dot. A natural candidate would be the nearby edge channel of the MZI, “back acting” on the QD; however, increasing the current in the MZI, thus increasing its shot noise, didn’t increase  $\Gamma$  further. Another possibility is spin flip processes, due to hyperfine coupling with the nuclei, which will allow tunneling into the outer edge channel and then to the leads; the shorter dwell time in the dot will lead to an increased  $\Gamma$ . These assumptions must be backed by adequate theoretical understanding.

As a further test, we examined also the decoherence rate of the outer edge channel in the dot. In order to allow dwelling of the outer edge in the dot, we restricted transport in QDL and QDR further, thus fully reflecting the inner channel and partitioning the outer channel. Following the evolution of the conductance peaks and comparing them to the visibility peaks (namely, the coherent part of the conduction) as function of pinching the outer channel in the dot is expected to reveal the decoherence rate in the dot. The observed visibility can be expressed as a function of the dot’s transmission  $T_{\text{QD}}$ ,  $v = \xi \frac{2\sqrt{T_{\text{QD}}}}{1+T_{\text{QD}}} \bar{v}$ , with  $\xi$  a phenomenological decoherence factor, and  $\bar{v}$  the bare visibility of the MZI, namely, without an embedded QD. As seen in the inset of Fig. 4 the decoherence rate, expressed by  $\xi$ , drops monotonically with pinching the outer channel. For an estimated  $\tau_{\text{dwell}} > 1$  ns, decoherence dominates (i.e.,  $\Gamma_{\text{elas}} \ll \Gamma_{\text{inelas}}$ )—in accordance to previously published works [11].

We presented here a study of two coupled interferometers, one an electronic Mach Zehnder interferometer and the other an electronic Fabry-Perot interferometer in a form of a QD weakly coupled to its leads. This coupled system allowed a unique and simple manifestation the Friedel sum rule, which explains the observed universal, and robust,  $\pi$  phase slips in the interference pattern in the MZI due to Coulomb interaction with the QD interferometer. Four noteworthy aspects of the experiment should be stressed. (i) The MZI proved to be an accurate detector of the average charge occupation and its fluctuations in the coupled QD. Although similar detection of occupation of a QD had been performed before with a QPC detector [1,12,13], the MZI’s great sensitivity-independent of the current it supported allowed detailed and sensitive detection, in the linear and nonlinear regimes, in a highly robust manner. (ii) Unexpectedly, the presence of the QD, merely at equilibrium (no current flowing), was sufficient to fully dephase the interferometer at 45 mK. This is in stark contrast to previous works, where dephasing of the interferometer required partitioned currents carrying large shot noise. (iii) While the QD fully dephased the MZI, the reciprocal process, due to “backaction” of the MZI on the QD was not observed [14]. This apparent lack of reciprocity can be attributed, in the case of the QD being coupled to the leads, to the rather limited dephasing of the

MZI; hence, any backaction (that may lead to broadening of the conductance peaks of the QD) is also expected to be very small. Alternatively, in the case of a pinched QD, broadening of the peaks is dominated by temperature or naturally higher  $\Gamma$  (due to decoherence or current leaking out of the dot), masking any broadening due to backaction. (iv) Presently, it is not clear what the role of temperature is and whether dephasing will occur at strictly zero temperature. On one hand, in the absence of thermal noise or shot noise, the QD will not induce phase fluctuations in the MZI; thus, no dephasing will take place; however, since the MZI must be (even though slightly) out of equilibrium in order to observe electron interference via transport measurements, energy can be transferred to the QD and thus back act on the interferometer, leading thus to self-dephasing of the MZI. This is a delicate matter that has been discussed in a recent Letter by Rosenow and Gefen [15].

We thank Oktay Göktaş for his contribution and Yuval Oreg, Yunchul Chung, Bernd Rosenow, Yoseph Imry, Izhar Neder, and Assaf Carmi for helpful discussions. M. Heiblum and Y. Gefen acknowledge the partial support of the Israeli Science Foundation (ISF), the Minerva foundation, and the U.S.-Israel Bi-National Science Foundation (BSF). M. Heiblum acknowledges also the support of the European Research Council under the European Community's Seventh Framework Program (FP7/2007-2013)/ERC Grant agreement No. 227716, the German Israeli Foundation (GIF) and the German Israeli Project Cooperation (DIP).

\*To whom all correspondence should be addressed.  
moty.heiblum@weizmann.ac.il

- [1] E. Buks, R. Schuster, M. Heiblum, D. Mahalu, and V. Umansky, *Nature (London)* **391**, 871 (1998).
- [2] D. Sprinzak, E. Buks, M. Heiblum, and H. Shtrikman, *Phys. Rev. Lett.* **84**, 5820 (2000).
- [3] I. Neder, M. Heiblum, D. Mahalu, and V. Umansky, *Phys. Rev. Lett.* **98**, 036803 (2007).
- [4] L. Meier, A. Fuhrer, T. Ihn, K. Ensslin, W. Wegscheider, and M. Bichler, *Phys. Rev. B* **69**, 241302 (2004).
- [5] S. C. Youn, H. W. Lee, and H. S. Sim, *Phys. Rev. B* **80**, 113307 (2009).
- [6] Y. Ji, Y. Chung, D. Shprinzak, M. Heiblum, D. Mahalu, and H. Shtrikman, *Nature (London)* **422**, 415 (2003).
- [7] See Supplemental Material at <http://link.aps.org/supplemental/10.1103/PhysRevLett.109.250401> for non-linear regime behavior and supporting results.
- [8] L. P. Kouwenhoven, D. G. Austing, and S. Tarucha, *Rep. Prog. Phys.* **64**, 701 (2001).
- [9] J. S. Langer and V. Ambegaokar, *Phys. Rev.* **121**, 1090 (1961).
- [10] C. W. J. Beenakker, *Phys. Rev. B* **44**, 1646 (1991).
- [11] J. A. Folk, C. M. Marcus, and J. S. Harris, *Phys. Rev. Lett.* **87**, 206802 (2001).
- [12] M. Avinun-Kalish, M. Heiblum, O. Zarchin, D. Mahalu, and V. Umansky, *Nature (London)* **436**, 529 (2005).
- [13] S. Gustavsson, R. Leturcq, M. Studer, T. Ihn, K. Ensslin, D. C. Driscoll, and A. C. Gossard, *Nano Lett.* **8**, 2547 (2008).
- [14] A. Stern, Y. Aharonov, and Y. Imry, *Phys. Rev. A* **41**, 3436 (1990).
- [15] B. Rosenow and Y. Gefen, *Phys. Rev. Lett.* **108**, 256805 (2012).